

Soft-tissue material properties under large deformation: Strain rate effect

Tie Hu, Jaydev P. Desai*

Program for Robotics, Intelligent Sensing, and Mechatronics (PRISM) Laboratory
Drexel University, Philadelphia, PA 19104
Email: {tie, desai}@coe.drexel.edu

Abstract: Biomechanical model of soft tissue derived from experimental measurements is critical for developing a reality-based model for minimally invasive surgical training and simulation. In our research, we have focused on developing a biomechanical model of the liver with the ultimate goal of using this model for local tool-tissue interaction tasks and providing feedback to the surgeon through a haptic display. In this paper, we are interested in finding the local effective elastic modulus (LEM) of the liver tissue under different strain rates. We have developed a tissue indentation equipment for characterizing the biomechanical properties of the liver and compared the local effective elastic modulus (LEM) derived from experimental data with plane stress, plane strain, and axisymmetric element types in ABAQUS under varying strain rates. Our results show that the experimentally derived local effective modulus matches closely with the plane stress analysis in ABAQUS.

Keywords—Tissue characterization, Local Effective Modulus, Liver Modeling, Surgical Simulator.

I. INTRODUCTION

In surgery, probing soft tissue is one of the most common tasks to ascertain the tissue characteristic as being hard or soft. Hence, reality-based modeling of soft tissues is critical for providing accurate haptic feedback to the surgeon in surgical training and simulation. By reality-based modeling, we are interested in modeling tissues as accurately as possible by determining the mechanical properties experimentally. The goal of this paper is to derive the local effective modulus (LEM) of the liver tissue as it is compressed over a large range at different strain rates. In our study, pig liver was used as the sample tissue for deriving the material properties. The technique developed in this paper can be easily extended to characterize the material properties of other soft tissue as well.

“Global” elastic deformations of real and phantom tissues have been studied extensively in previous work, through simple poking interactions [1]. However, these methods are simplistic since they do not consider the complex boundary conditions that are normally present, both internal to the organ and on the exterior surface. Howe and colleagues [2] have developed a “truth cube” for validation of models, however they have not yet extended this model to tool-tissue interactions for common surgical tasks such as probing tissues. There has also been research on estimating the mechanical properties of the tissue through high-frequency shear deformations of the tissue sample, and elastography techniques. A variety of other techniques also exist in the literature for estimating the viscoelastic characterization of tissues, for example, [3] [4].

Ottensmeyer [5] and others have performed tissue experiments to characterize force vs. displacement for pig liver tissue, however the tissue displacement was small and they have not characterized the mechanical properties of the liver.

In general, soft tissue is compressible, non-homogeneous, non-isotropic and viscoelastic. However, it can be treated as a “pseudo-elastic” material [6] when it is compressed or stretched. We have studied the LEM of the liver tissue under the quasi-static status [7]. In this paper, we want to study the LEM of the liver tissue under varying strain rates. In real surgery, the surgeons probe the tissue over a large range and they do not precondition the tissue before probing. As a result all our analysis is on non-preconditioned tissue to developing a realistic model. The material characterization of the liver tissue under varying strain rates thus has practical significance in developing a surgical simulator. We built a finite element model to simulate the experimental process.

The rest of this paper is organized as follows. In section 2, we describe the materials and methods used to derive LEM for the liver over a large deformation range. We present the computational method in ABAQUS to derive the LEM over the range of deformation using plane stress, plane strain, and axisymmetric element types. In section 3, we present our experimental results and compare them with ABAQUS model at varying strain rates. Finally in section 4, we make some concluding remarks and discuss our future work in this area.

II. METHODOLOGY

2.1 Experimental Setup

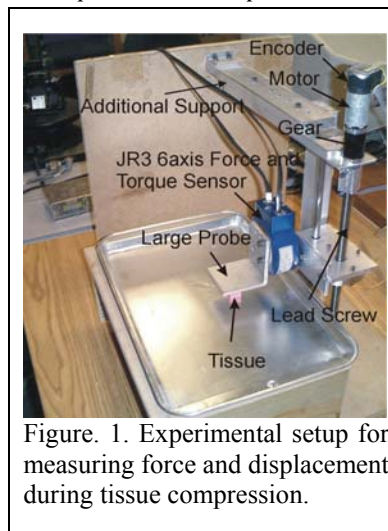


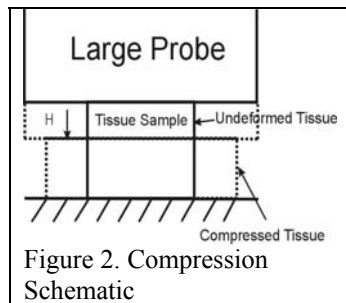
Figure. 1. Experimental setup for measuring force and displacement during tissue compression.

We have designed and developed a tissue compression apparatus, which can measure the compressive force and displacement. Figure 1 shows the configuration of our experimental system. The system consists of a motion control part, a force measuring part, and a post-data processing part. The motion control part is a lead screw assembled

*Corresponding Author.

with a geared DC motor and encoder (Maxonmotor, Inc. A precision JR3 6 axis force/torque sensor (model 85M35A-140) was attached to the probe. The position and velocity of the probe was controlled by the dSPACE DS1103 controller board (dSPACE, Inc.) and it also records the force and displacement data. The size of the probe was 50mm x 50 mm and the surface was polished and covered with petroleum jelly to minimize the contact friction force. The size of the probe ensured that the liver sample fully contacted with the probe surface and contact over the entire surface was maintained. We also assumed that over the entire range of compression the volume of the sample was conserved (though in reality this is not generally true). The liver samples were taken from freshly slaughtered pigs and transported to the lab within 2 hours post mortem. We made a tube (25.4 mm diameter) with sharp edge and used it to prepare the cylindrical sample (22.2mm in diameter and 13mm in height). The probing speeds for our experiments ranged from 1.27mm/sec to 25.4mm/sec.

2.2 Large Probe Model



In surgery, the surgeon probes the tissue with a probe, which is significantly smaller than the organ surface. However, from an analysis viewpoint, small probe analysis introduces significantly complicated boundary conditions and

the corresponding analytical problem is difficult to solve. We hypothesize that the first step to develop a numerical model for the small probe is to characterize the material property by large probe analysis and use that model as an initial guess in the iterative numerical computation for small probe analysis. In a larger probe analysis, the probe is larger than the sample so that the deformation of the sample is uniform and the boundary country is simple. Hence, the stress and strain relationship characterizing the material property can be obtained from the experimental force and displacement data.

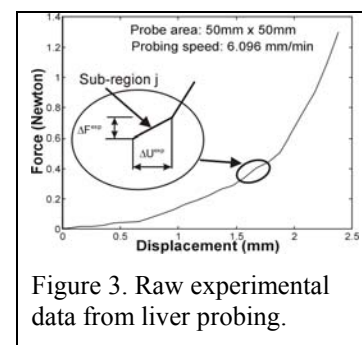


Figure 3. Raw experimental data from liver probing.

Figure 2 shows the schematic of the large probe compression test. In our analysis we assume that the tissue is incompressible, isotropic, and homogenous elastic material. We derive the experimental stress and strain relationship based on our force-

displacement data for large probe compression of soft tissue. To calculate the LEM, we divide the whole deformation into 30 sub-regions; each of them has a 1% strain increment. We

analyze each sub-region as consisting of a linear deformation characterized by a unique LEM value. Hence, we get a sequence of LEM values for each test over the range of tissue compression. In this paper we are interested in finding the effect of the strain rate on the LEM value for the pig liver tissue.

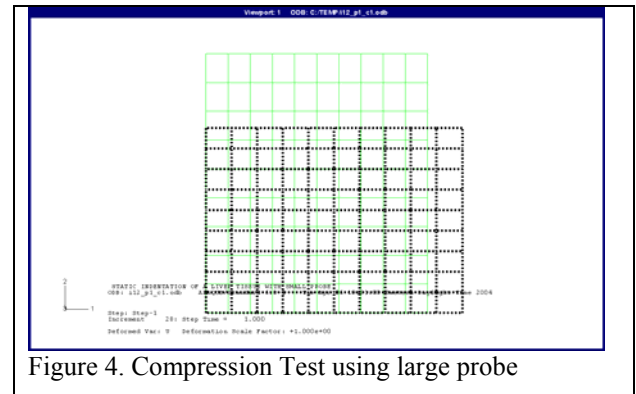


Figure 4. Compression Test using large probe

2.3 Finite Element Modeling (ABAQUS)

It is desirable to construct a predictive computational model that can simulate the tissue probing process and predict the mechanical response (probing force versus displacement characteristics) of liver probing. We propose to use two-dimensional finite element (FE) models for this purpose. The force and displacement data for the strain rate 1.27 mm/sec, 2.54 mm/sec and 25.4 mm/sec were experimentally obtained. For each data, the LEM for the certain strain rate could be obtained by using the following method.

A 2D finite element model was built in ABAQUS (Release 6.3-1) to simulate the compression process and iteratively obtain the computational LEM under a certain strain rate. Figure 4 shows the corresponding deformed and un-deformed model in ABAQUS during tissue compression. Since the sample is cylindrical, it is symmetric with the central line. The geometry of the model takes the left side of the sample and the left line is horizontally constrained. The top of the model is constrained with a displacement boundary condition, which functions as a rigid probe. The displacement on the top of the model is probing displacement. The sum of the nodes reaction force on the top of the model is the probing force. The bottom of the model is vertically constrained. The material property of the model is linear. Total element numbers are 90. Three element types, plane stress, plane strain, and axisymmetric were tested separately to find the local effective modulus. The element types separately were CPE4, CPS4 and CAX4 in ABAQUS.

The whole deformation was divided into 30 sub-regions. Each region can be considered as liner deformation, which can be characterized by a local effective modulus. The modulus of a biological tissue is a measure of its deformation resistance. It is not constant and it can vary from location to location. For the large deformation, the deformed geometry has an obvious effect on the strain, i.e.,

as the tissue is progressively deformed the history of deformation has an effect on the modulus at a given displacement of the tissue. Thus in the ABAQUS formulation, for any given sub-region j ($j=1,2,\dots$) of the force vs. displacement curve, the current geometry of the deformed mesh has to be imported into the model from the previous step to compute the values for the new linear region. This was accomplished by using the IMPORT option in ABAQUS, which allows us to import the geometry and the mesh of the model. The initial stress for each increment was set to zero because the initial stress doesn't have effect on the local effective E modulus for the increment (due to plane stress and plane strain analysis). We assumed Poisson's ratio of 0.3 and an initial LEM of arbitrary magnitude $E_{1,j}$ to start the simulation. Then the experimentally measured displacement ΔU^{EXP} was applied to the node that models the large probe. The linear FE analysis was performed and the FE-computed reaction force ΔF^{FEM} of that node was compared with the experimentally measured ΔF^{EXP} . The E value is updated by equation (1) until ΔF^{FEM} of the new iteration converged to the experimentally measured ΔF^{EXP} as per the convergence criterion given by Equation (2). The converged value for the local effective modulus was denoted as $E^{effective}$ for that region.

$$E_{i+1,j} = E_{i,j} \left(\frac{\Delta F^{EXP}}{\Delta F^{FEM}} \right) \text{ for } i,j=1,2,\dots \quad (1)$$

$$\frac{\|\Delta F_j^{FEM} - \Delta F_j^{EXP}\|}{\Delta F_j^{EXP}} \leq 0.02 \text{ for } j=1,2,\dots \quad (2)$$

The first subscript, i , of $E_{i,j}$ is the iteration number in each

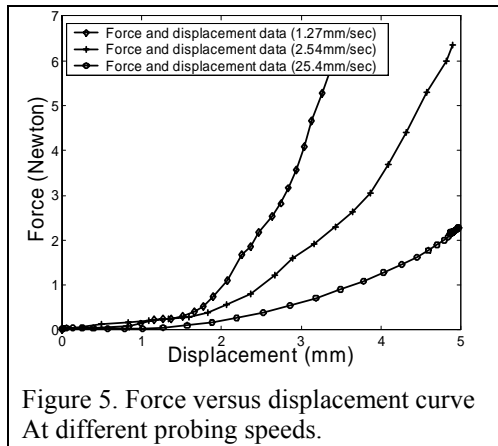


Figure 5. Force versus displacement curve At different probing speeds.

sub-region, and the second subscript, j , of $E_{i,j}$ is the sub-region number.

Once E_j is computed for a sub-region j , this was the initial input value of

E_{j+1} (for

the next sub-region $j+1$). The deformed geometry and the meshes for the sub-region j are imported into the model for the sub-region $j+1$ and the process is repeated until the final sub-region is analyzed. It is very important to use the IMPORT option to import the model geometry, since the deformed geometry has a significant effect on the strain in large deformation regions. A program using Python script language was used to automatically update the E modulus. The local effective modulus $E^{effective}$ so determined is a

measure of the deformation of the tissue consistent with the experimental data and the FE discretization.

III. RESULTS

3.4 Comparison of LEM at different strain rates

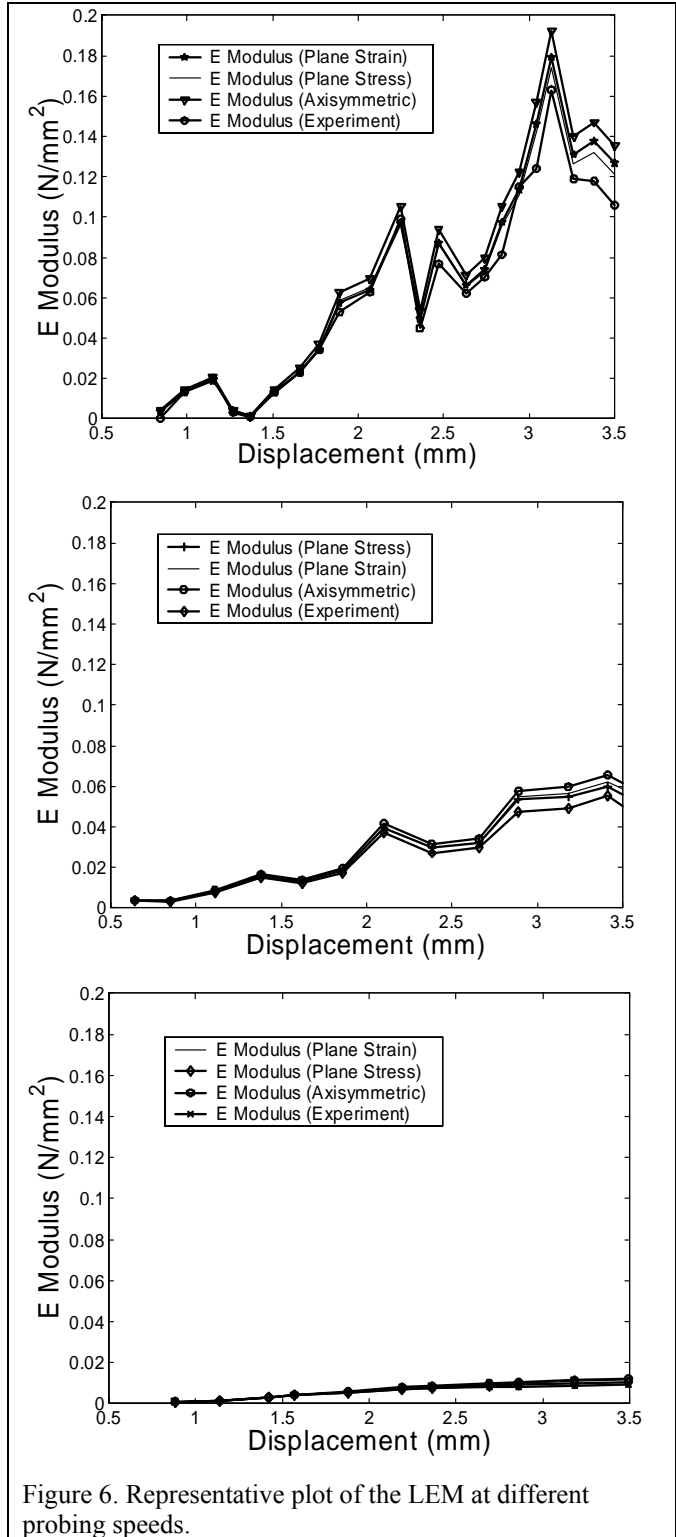


Figure 6. Representative plot of the LEM at different probing speeds.

In surgery, surgeons probe the liver tissue with variable speed over a large range. In this paper, we were interested in studying the variation of LEM of pig liver tissue at different strain rates. To realistically simulate the probing process, we used three probing speeds, namely, 1.27 mm/sec, 2.54 mm/sec and 25.4 mm/sec. The highest speed was chosen to simulate normal probing speed of the surgeon. The slowest speed was chosen to perform quasi-static analysis. For each strain rate, we did 5 trails. Figure 5 shows the representative force and displacement data for different compression speeds. The data was filtered with a low-pass filter after it was obtained from the experiment. We however did not do curve fitting since we wanted to preserve the realistic tissue behavior for LEM computation. As shown in the plot, the force versus displacement plot is significantly “flatter” at higher probing speeds compared to the quasi-static case (1.27mm/sec). This characteristic shows that the pig liver at higher strain rates has an apparently lower resistance to deformation than at lower strain rates.

Figure 6 shows the representative plot of the LEM computed with 1% strain increment at different strain rates, namely, 1.27mm/sec, 2.54mm/sec, and 25.4 mm/sec. Three computational models using plane stress, plane strain and axisymmetric elements were used to calculate the LEM in ABAQUS. The result shows that the computational modulus is close to the experimental modulus at the highest probing speed for all three element types. However at lower probing speeds, the plane stress model is closet to the experimental modulus among the three computational models. From the plot, we also observe that the LEM at low strain rate is greater than the LEM at a higher strain rate. As a result, we can conclude that the apparent resistance to deformation of the soft tissue is higher at lower probing speeds compared to higher probing speeds.

IV. CONCLUSION

We have developed a tissue probing apparatus whereby we can control the probing speed and acquire the force versus displacement information of the soft-tissue. In our analysis, we assumed a large probe model whereby the probe was larger than the tissue. We performed experiments at three different strain rates to understand the effect of the strain rate on the local effective modulus of the tissue as it is compressed. The highest probing speed was chosen to be 25.4mm/sec (1in/sec) to simulate normal probing by the surgeon of the soft -tissue. We compared the experimental stress vs. strain data with the ABAQUS model for three different element types, namely, plane stress, plane strain, and axisymmetric. Our analysis reveals that the plane stress model fits better with the experimental data at lower strain rates and at higher strain rates all the element types fit well. Our analysis assumed that the tissue was incompressible, isotropic, and homogenous. However, in reality this is not valid. Hence, our future work in this area will involve developing a more complex model for the soft-tissue.

ACKNOWLEDGMENT

The authors would like to acknowledge the support of National Science Foundation grants EIA-0312709 and CAREER award IIS-0133471 for this work.

REFERENCES

- [1] d'Aulignac, D., R. Balaniuk, and C. Laugier, *A Haptic Interface for a Virtual Exam of the Human Thigh*. Proceedings of the IEEE International Conference on Robotics & Automation, 2000: p. 2452-2456.
- [2] Kerdok, A.E., *Soft Tissue Characterization: Mechanical Property Determination from Biopsies to Whole Organs*. Whitaker Foundation Biomedical Research Conference, 2001.
- [3] Arbogast, K.B., *et al.*, *A High-Frequency shear device for testing soft biological tissues*. Journal of Biomechanics, 1997. **30**(7): p. 757-759.
- [4] Halerpin, H.R., *et al.*, *Transverse Stiffness: A methods for Estimation of Myocardial Wall Stress*. Circulation Research, 1987. **61**(5): p. 695-703.
- [5] Ottensmeyer, M.P., *In vivo measurement of solid organ viscoelastic properties*. Medicine Meets Virtual Reality, 2002. **2**(10): p. 328-333.
- [6] Fung, Y.C., *Biomechanics: Mechanical properties of living tissues*. Second edition ed. 1993, New York: Springer-Verlag.
- [7] Hu, T. and J.P. Desai, *Characterization of soft-tissue material properties: Large deformation analysis*. International Symposium on Medical Simulation.2004, Cambridge, MA.